The characteristics of heat-driven ammonium adsorption in aerobic granular sludge

Junguo He and Jie Xu

ABSTRACT

Adsorption is an important step during the migration of ammonium from the aqueous phase to biomass in biological nitrogen removal processes. A deeper understanding of the adsorption mechanisms is encouraged in constructing nitrogen conversion models. In this study, the ammonium adsorption in aerobic granular sludge was investigated at different conditions. Analysis of kinetic data indicated that ammonium adsorption was a fast process and followed pseudo-second-order kinetics (adsorption rate constant k_2 was between 0.031 and 0.065 g/(mg · min)). The maximum adsorption capacity and half saturation constant K_L in the Langmuir isotherm model were 4.95 mgNH_4^+-N/g total suspended solids and 0.0126 L/mg, respectively. Effects of environmental conditions such as temperature, pH and competitive cations were also estimated. The optimum pH was 7 and the effects of competitive cations were in the order $Ca^{2+} > Mg^{2+} > K^+ > Na^+$. Values of thermodynamic parameters ($\Delta H^{\Theta} = -14.697$ kJ/mol, $\Delta S^{\Theta} = -6.65$ J/(mol · K)) indicated that the adsorption process was spontaneous and exothermic. Desorption tests showed that the process was reversible and low temperature had a negative effect on ammonium desorption. These findings could be useful for completing the mathematical model of the nitrogen removal process in bioreactors.

Key words | aerobic granular sludge, ammonium adsorption, desorption, isotherm, kinetic

Junguo He (corresponding author)
Jie Xu
School of Environment,
Harbin Institute of Technology (HIT),
Second campus of HIT, No.73 Huanghe Road,
Nangang District, Harbin 150090,
China
E-mail: *hejunguohit@126.com*

INTRODUCTION

Nitrogen is an essential component for all kinds of life, but is also a source of eutrophication, a worldwide environmental challenge (Gooddy *et al.* 2016). Various methods have been used for the removal of nitrogen in traditional municipal and industrial wastewater treatment plants (WWTPs). Among them, biological processes might be the most commonly employed, in which the nitrogen is mainly removed through nitrification and denitrification, two important processes accomplished by converting ammonium to nitrate and then reducing to nitrogen gas in multi-step reactions.

Aerobic granular sludge (AGS) is a form of microorganic self-flocculation aggregation with a dense structure, abundant biomass and high pollutant removal rate compared with conventional activated sludge (de Kreuk *et al.* 2005). Diffusion of dissolved oxygen is limited due to the special layered structure of AGS. In turn, the aerobic, anoxic and anaerobic zones are formed, providing suitable growth conditions for nitrifying and denitrifying bacteria, which allows simultaneous nitrification and denitrification (Mosquera-Corral *et al.* 2005). In this case, the AGS technology has a greater advantage in the treatment of high- or low-intensity nitrogen wastewater. (Corsino *et al.* 2016; Drzewicki *et al.* 2017; Zou *et al.* 2018). Researchers have studied the transformation of nitrogen in AGS (Zhou *et al.* 2013). However, the quantitative calculation of nitrogen conversion and mass balance is an arduous task because there are numerous parallel conversion processes during nitrogen removal (Van Loosdrecht & Jetten 1998).

In the process of nitrogen transformation, ammonium adsorption in microbial aggregation is an important part which has not been paid much attention. Nielsen (1996) discovered the ammonium adsorption phenomenon for the first time while extracting ammonium from activated sludge using potassium chloride solution. The extractable amounts were 0.5–1.3 mgNH_4^+-N/L higher when the dissolved ammonium concentrations were between 1 and 6 mgNH_4^+-N/L. Adsorption experiments showed that about 2 mg/L ammonium was adsorbed when the bulk concentration was around 15 mgNH_4^+-N/L, corresponding to

doi: 10.2166/wst.2018.418

adsorption capacity of 0.3–0.4 mgNH_4^+-N/g suspended solids. Wik (1999), in a study examining the nitrification and denitrification processes in a pilot-scale nitrifying trickling filters reactor, found that ammonium could be adsorbed and desorbed by biofilm. The highest adsorption capacity was 2.7 mgN/m^2 when the influent ammonium concentration was around 15 mgNH_4^+-N/L. Schwitalla *et al.* (2008) observed that the adsorption capacity of activated sludge on ammonium was between 0.07 and 0.20 mgNH_4^+-N/g volatile suspended solids (VSS) in full-scale sequencing batch reactor (SBR) WWTPs. The NH_4^+-N adsorption/desorption was inversely associated with K^+ adsorption/desorption. Bassin *et al.* (2011) compared the ammonium adsorption in AGS, activated sludge and anammox granules. Adsorption capacities of lab- and pilot-scale AGS were 1.7 and 0.9 mgNH_4^+-N/gVSS, while only 0.2 mgNH_4^+-N/gVSS was obtained in anammox granules and activated sludge. Li *et al.* (2016) studied the ammonium adsorption in anammox granular sludge and found that the process was spontaneous and exothermic. The Freundlich isotherm described the ammonium adsorption process well. In general, the microbial cell surface and extracellular polymeric substances (EPS) carry a negative charge; therefore ammonium or other cations could be adsorbed through electrostatic adherence or ion exchange (Bassin *et al.* 2011). The specific surface area of AGS is high and its structure is far more complex compared with activated sludge (Zhang *et al.* 2005). These might improve the adsorption capacity of ammonium in AGS and they cannot be neglected when considering the nitrogen removal process. Therefore, it is necessary to conduct a further study into the ammonium adsorption process in AGS.

Herein, we studied the adsorption/desorption properties of AGS on ammonium. The adsorption kinetics, isotherm models and thermodynamics analysis were used to clarify the ammonium adsorption process. Meanwhile, parameters affecting the adsorption such as temperature, pH and co-existing cations were further investigated. Our findings could be useful for completing the mathematical model of the nitrogen removal process in AGS.

MATERIAL AND METHODS

Cultivation of aerobic granular sludge

AGS was collected from a lab-scale SBR operated at 20 ± 0.5 °C which was fed with synthetic wastewater with the following composition: NaAc 6.1 mmol/L, NH_4Cl 3.57 mmol/L, K_2HPO_4 0.34 mmol/L, KH_2PO_4 0.17 mmol/L, $MgSO_4 \cdot 7H_2O$ 0.3 mmol/L, KCl 0.38 mmol/L and 1 mL/L trace element solution according to Vishniac & Santer (1975). This gave rise to ammonium concentration of 50 mgNH_4^+-N/L and chemical oxygen demand of 400 mg/L, respectively. The working volume of the reactor was 2.0 L with an internal diameter of 6.0 cm and a total height of 100 cm. The cycle time was 4 h with 60 min anaerobic feeding from the bottom of reactor, 172 min aeration provided by a fine-bubble aerator, 3 min settling and 5 min effluent withdrawal. Dissolved oxygen concentration was nearly saturated during aeration phase while the aeration rate was 2.67 L/min with a superficial gas velocity of 1.57 cm/s. The volume exchange ratio was 0.5, corresponding to a hydraulic retention time of 8.0 h. The pH in the reactor was controlled at 7.0 ± 0.2 through dosing HCl and NaOH solution. The reactor had been running stably for 1 year before the sorption experiments started. Average particle size of AGS has been around 1.5 mm since the reactor was successfully started up.

Adsorption/desorption batch tests

Adsorption tests were carried out in 250 mL blue cap bottles using AGS collected from the SBR at the end of an operational cycle. Tris-HCl buffer (0.1 M, pH 7) was utilized to wash the AGS three times to remove residual ammonium. The bottles were shaken at 160 rpm for 90 min and the temperature was kept at 20 ± 0.5 °C. Two types of experiments were conducted to test the adsorption ability of AGS on ammonium: one varying the ammonium concentrations from 25 to 115 mgNH_4^+-N/L while keeping the sludge concentration at 5 g/L and the other varying the sludge concentrations from 1.5 to 10 g/L while keeping the initial ammonium concentration at 50 mgNH_4^+-N/L. The systems were purged using high purity nitrogen (99.99%) for 5 min and then sealed with rubber plugs before adding ammonium. Syringes were used to take samples at different time intervals to keep the environment anaerobic.

Desorption tests were carried out in two steps. Firstly, adsorption tests were conducted as described above, in which the concentrations of sludge and initial ammonium were controlled at 5 g/L and 50 mgNH_4^+-N/L, respectively. After that, samples were taken to estimate the amount of ammonium adsorbed on granules. Then, these granules were sieved to remove all the liquid and transferred to blue cap bottles which had been filled with 0.1 M Tris-HCl buffer (pH 7) and purged utilizing high purity nitrogen to get an anaerobic state. The bottles were shaken at different temperatures respectively while keeping the rotational

speed and time the same as for the adsorption experiments. The equilibrium ammonium concentrations in liquid after desorption were measured and the desorption rate was estimated to identify the effect of temperature on the desorption process and whether the adsorption is reversible.

Effects of environmental factors

To investigate the effects of different environmental factors on ammonium adsorption, experiments were performed keeping the initial ammonium and sludge concentration at 50 mgNH_4^+-N/L and 5 g/L, respectively. The bottles were shaken at 160 rpm for 90 min. The influence of temperature was studied over a range of 10–40 °C while other experiments were conducted at a temperature of 20 ± 0.5 °C. The pH was kept at 7.0 ± 0.2 except when evaluating the pH effect on ammonium adsorption, in which a pH range of 5.0–9.0 in 1.0 unit increments was applied. Sodium (Na^+), potassium (K^+), magnesium (Mg^{2+}) and calcium (Ca^{2+}) were chosen as the co-existing cations because they are the most common cations in various types of wastewater including municipal and industrial wastewater, which could compete with ammonium for adsorption sites. All of the operating and changing parameters in the adsorption and affecting factors experiments are shown in Table S1 (available with the online version of this paper).

Granular characterization, chemical analysis and calculation procedures

The Fourier transform infrared (FTIR) spectrum of AGS was analyzed to identify the functional groups using an FTIR spectrometer (USA) in the range of 4,000 to 450 cm^{-1}. The microstructure of AGS was obtained using a Hitachi SU8010 scanning electron microscope (SEM) coupled with energy dispersive X-ray spectrometry (EDS). Total suspended solids (TSS) and ammonium concentrations were determined according to standard methods (APHA 1998). Temperature and pH were determined by an HI 8424 pH meter.

The amount of ammonium adsorbed by AGS at equilibrium state (q_e) and desorption efficiency (η) could be calculated according to the following equations:

$$q_e = \frac{C_o - C_e}{TSS} \quad (1)$$

$$\eta = \frac{C_{eq}}{C_o - C_e} \times 100\% \quad (2)$$

where C_o and C_e are the initial and equilibrium ammonium concentrations in the solution (mgNH_4^+-N/L). TSS is the total suspended solids (g/L). C_{eq} is the equilibrium ammonium concentration after desorption (mg/L).

RESULTS AND DISCUSSION

Characteristics of AGS

The FTIR spectrum of AGS is illustrated in Figure 1. The O-H stretching vibration appeared at 3,329 cm^{-1}. The stretching vibration absorption of C-H was observed at 2,925 cm^{-1}, representing aliphatic compounds. Asymmetric $-COO^-$ stretching vibration appeared at 1,551 cm^{-1}, indicating that the AGS carried a negative charge. Groups of amide compounds appeared at 1,660 and 1,407 cm^{-1}, which were confirmed to be stretching vibration of C=O and deformation vibration of N-H, respectively. The adsorption peaks of C-O in polysaccharide compounds were observed at 1,245 and 1,057 cm^{-1}.

Figure S1 shows the SEM pictures of the structure of AGS obtained from the SBR. An irregular sphere with abundant channels, which contributed to the diffusion of ammonium ions, was observed (Figure S1(a)). The surface of granules shown in Figure S1(b) reveals that the surface of AGS was lumpy with plenty of micropores, which may provide a large number of adsorption sites and facilitate the diffusion of ammonia ions. Closer observation indicated that coccus was the dominant bacteria in AGS as shown in Figure S1(c). According to the EDS analysis shown in Figure S2, several metal cations were contained in the surface of AGS, which provided ion exchange sites for ammonium ions. (Figures S1 and S2 are available with the online version of this paper.)

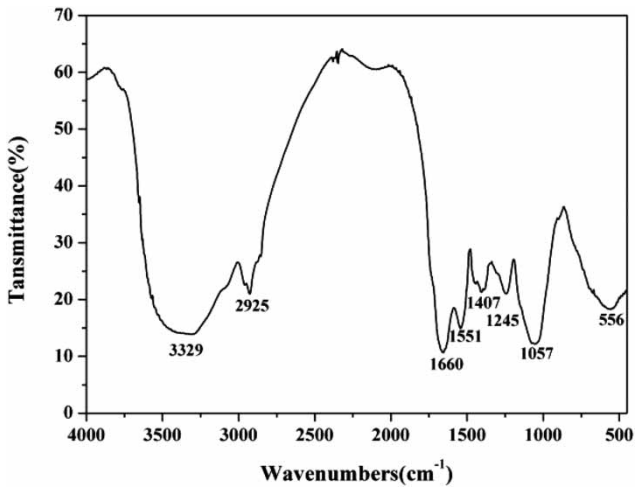

Figure 1 | FTIR spectrum of AGS.

Adsorption kinetics

Adsorption properties of AGS at different initial ammonium concentrations or sludge concentrations were tested and the data are presented in Figure S3(a) and 3(b). Similar to the results of Bassin *et al.* (2011), a rapid decrease in ammonium concentration was noted at the beginning of both experiments and the adsorption rate decreased gradually. Adsorption equilibrium was mostly reached within 60 min, indicating that the adsorption process was fast. Generally speaking, the adsorption process in liquid is controlled by the diffusion velocity and adsorption rate on the surface and internal channels of adsorbent particles (Liu *et al.* 2010). As the ammonium concentrations increased from 25 to 115 mgNH_4^+-N/L, the diffusion rate of ammonium ion was increased, and so was the collision chances between ammonium ions and adsorption sites in AGS, resulting in a higher adsorption rate compared with low ammonium concentrations. The collision chances could also be improved by increasing sludge concentration as there would be more adsorption sites provided. However, the adsorption rate of AGS was decreased from 2.92 to 1.86 mgNH_4^+-N/(gTSS · h) when sludge concentration increased from 1.5 to 10 g/L, as shown in Figure S4. This might be caused by a stronger cell shadowing effect which produced a higher block of the cell active sites at higher biomass concentration (Hammaini *et al.* 2007). (Figures S3 and S4 are available online.)

In order to further determine the adsorption kinetics of AGS on ammonium, the Lagergren pseudo-first-order kinetic model (Equation (3)), Blanchard pseudo-second-order kinetic model (Equation (4)) and Elovich model (Equation (5)) were applied. The Weberen Morris intra-particle diffusion model (Equation (6)) was also investigated to determine the key steps that control the ammonium adsorption process.

$$\lg(q_e - q_t) = \lg q_e - \frac{k_1 t}{2.303} \tag{3}$$

$$\frac{t}{q_t} = \frac{1}{k_2 q_e^2} + \frac{1}{q_e} t \tag{4}$$

$$q_t = A + B \ln t \tag{5}$$

$$q_t = K_d t^{\frac{1}{2}} + C \tag{6}$$

where t is the contact time (min), q_t is the adsorption capacity of AGS at time t (mg/g), k_1 is the adsorption rate constant of the Lagergren model (min^{-1}), k_2 is the adsorption rate constant of the Blanchard model (g/(mg·min)), K_d is the intra-particle diffusion rate constant (mg/(g·$min^{1/2}$)), A and B are the kinetic constants of the Elovich model and C is the constant that expresses the boundary layer thickness (Angar *et al.* 2016).

The adsorption experimental data in different initial ammonium concentrations were fitted to kinetic models. Results of linear fitting are shown in Figure 2(a)–2(c). The kinetic parameters' value and 95% confidence intervals (95% CI) and the correlation coefficients (R^2) are shown in Table 1. According to the values of R^2, the pseudo-second-order model was the best one to describe ammonium adsorption kinetics in AGS, whose correlation coefficients were between 0.995 and 0.998. Correlation coefficients of the pseudo-first-order model were between 0.94 and 0.977, while in the Elovich model, they were between 0.877 and 0.969. In addition, the calculated values of ammonium adsorption capacity at equilibrium ($q_{e\text{-cal}}$) in the pseudo-second-order model were closer to the experimental data ($q_{e\text{-exp}}$) than those of the pseudo-first-order model. Theoretical adsorption rate constant K_2 estimated from the pseudo-second-order model was between 0.031 and 0.065 g/(mg·min), further confirming that the adsorption of ammonium ion onto AGS is a fast process.

The ammonium adsorption kinetics in different sludge concentrations could also be well described by the pseudo-second-order model, as shown in Figure S5 and Table S2 (available online), for which the correlation coefficients were between 0.995 and 0.999. The pseudo-first-order model and Elovich model were invalid for adsorption kinetics here because of the low correlation coefficients. A pseudo-second-order suggests that the adsorption of ammonium onto AGS involves more than one step, and chemisorption including ion-exchange might be the main adsorption process (Ho & McKay 1999).

We next plotted q_t against $T^{1/2}$ using the adsorption data at different initial ammonium concentrations and the results are shown in Figure 2(d) and Table S3 (available online). It can be seen that the intra-particle diffusion model fits experimental data well and the diffusion curves exhibit two phases. Therefore, the diffusion of ammonium ion may depend on two stages. The first one defines ammonium ion diffusion from solution to the surface film layer of AGS and the calculated values of K_{d1} are big ($\geq$0.12), indicating a quick diffusion rate. The second stage is ammonium diffusion inside AGS and K_{d2} values are small ($\leq$0.041), suggesting that this process is slow. As a consequence, diffusion inside AGS could be considered to be the dominant process which controls ammonium diffusion rate. The shielding effect of EPS and microbial cells in the AGS makes the mass transfer resistance of ammonia ions

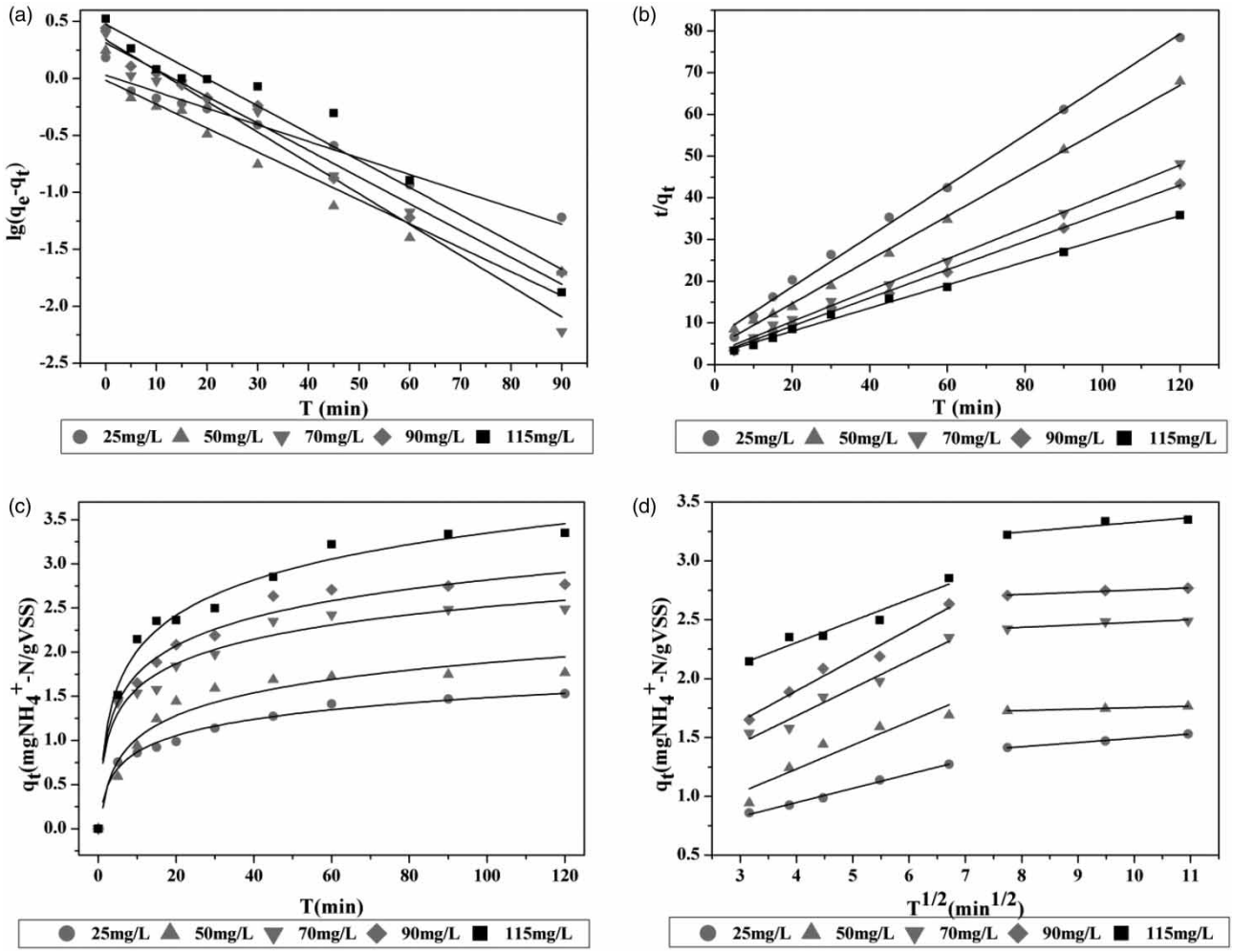

Figure 2 | Kinetic models of ammonium adsorption: (a) pseudo-first-order, (b) pseudo-second-order, (c) Elovich model and (d) intra-particle diffusion under different initial ammonium concentration.

inside the granules much larger than that on the external surface. In addition, the fitting lines of the intra-particle diffusion model do not pass through the origin point and the values of constants C_1 and C_2 were not zero, suggesting that the intra-granular diffusion is not the only process limiting the ammonium adsorption rate (Arami *et al.* 2008). In the bottles, ammonium ions can fully contact with AGS, so the diffusion in the surface liquid film layer could be neglected. Therefore, the rate control process might be the internal diffusion and surface adsorption.

Adsorption isotherms

Adsorption isotherms are the curves that describe the relationship between the quantity of adsorbate in system and adsorbent. In order to confirm the most suitable ammonium adsorption isotherm model in AGS, experimental data shown in Figure 3 were fitted to Langmuir, Freundlich and Temkin models which are given in Equations (7) to (9).

$$q_e = \frac{q_m K_L C_e}{1 + K_L C_e} \tag{7}$$

$$q_e = K_F c_e^{1/n} \tag{8}$$

$$\mathrm{q_e} = E\ln D + E\ln C_e \tag{9}$$

where q_e is the adsorption capacity at equilibrium (mg/g); C_e is the equilibrium concentration of ammonium in solution ($mgNH_4^+$-N/L); K_L is Langmuir constant (L/mg); q_m is the theoretical maximum adsorption capacity (mg/g); K_F is Freundlich constant (L/mg); n is the adsorption intensity; D is the equilibrium binding constant and E is Temkin constant.

Table 1 | Kinetic parameters for ammonium adsorption under different initial ammonium concentration

		C_o (NH_4^+) (mg/L)				
Kinetic models		**25**	**50**	**70**	**90**	**115**
Pseudo-first-order	$q_{e\text{-}cal}$ (mg/g)	1.071	0.966	2.193	2.056	2.998
	95% CI	±0.262	±0.210	±0.398	±0.372	±0.352
	$k_1(min^{-1})$	0.033	0.048	0.062	0.054	0.055
	95% CI ($\times 10^{-3}$)	±0.633	±1.23	±0.960	±0.902	±1.36
	R^2	0.966	0.94	0.977	0.973	0.942
Pseudo-second-order	$q_{e\text{-}cal}$ (mg/g)	1.649	1.911	2.671	2.961	3.608
	95% CI	±0.153	±0.231	±0.179	±0.255	±0.338
	k_2(g/(g·min))	0.056	0.065	0.049	0.045	0.031
	95% CI ($\times 10^{-3}$)	±0.955	±0.653	±0.495	±0.383	±0.416
	R^2	0.995	0.997	0.997	0.998	0.996
Elovich	A	0.252	0.166	0.665	0.686	0.682
	95% CI	±0.039	±0.112	±0.091	±0.088	±0.095
	B	0.268	0.372	0.402	0.463	0.579
	95% CI	±0.011	±0.032	±0.026	±0.025	±0.027
	R^2	0.969	0.877	0.927	0.948	0.96
$q_{e\text{-}exp}$ (mg/g)		1.531	1.746	2.489	2.767	3.35

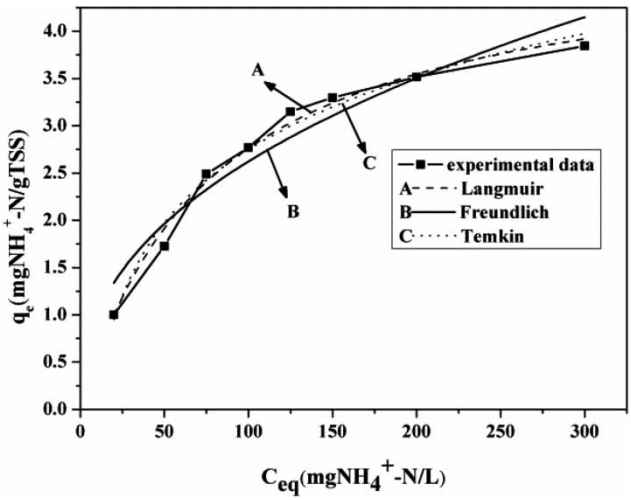

Figure 3 | Adsorption isotherms and fitted curves for ammonium adsorption.

The separation factor R_L can determine whether the adsorption of adsorbate is efficient. According to the R_L value determined by Equation (10), the adsorption can be divided into four types: favorable adsorption ($0 < R_L < 1$), unfavorable adsorption ($R_L > 1$); linear adsorption ($R_L = 1$) and irreversible adsorption ($R_L = 0$) (Zhao *et al.* 2010).

$$R_L = \frac{1}{1 + K_L C_o} \tag{10}$$

where K_L is Langmuir constant (L/mg) and C_o is the initial ammonium concentration (mgNH_4^+-N/L).

The Langmuir, Freundlich and Temkin plots for ammonium adsorption in AGS were obtained, and the fitting lines and parameters are shown in Figure 3 and Table 2. The curve of experimental data shows that the adsorption capacity increased rapidly at low ammonium concentration and the increment speed decreased gradually as ammonium concentration increased. The Langmuir model fits experimental data well as its correlation coefficient is higher than for Temkin and Freundlich models ($0.9879 > 0.9785 > 0.9231$), indicating that the adsorption of ammonium onto AGS is monolayer, with a theoretical maximum adsorption capacity of 4.95 mgNH_4^+-N/gTSS. Half saturation constant K_L is 0.0126 L/mg, lower than 1.0 L/mg, suggesting that the adsorption process is weak. The value of R_L lies between 0 and 1, which means that the adsorption of ammonium is favorable. This conclusion can also be proved by the empirical parameter $1/n$ in the Freundlich model, since its value of 0.418 is smaller than 1 (Raji & Anirudhan 1998). What is more, the R_L parameter

Table 2 | Estimated isotherm constants for ammonium adsorption

Parameters	**Langmuir**	**Freundlich**	**Temkin**
Parameter 1	$q_m = 4.95$	$n = 2.39$	$D = 0.117$
95% CI	±0.133	±0.371	±0.201
Parameter 2	$K_L = 0.0126$	$K_F = 0.383$	$E = 1.117$
95% CI	±0.001	±0.071	±0.043
R^2	0.9879	0.9231	0.9785

is closer to 0 when the initial concentration is big enough, suggesting that increasing ammonium concentration would be beneficial for adsorption.

Effect of temperature and adsorption thermodynamics

The effect of temperature on ammonium adsorption in AGS was conducted at 10, 15, 20, 25, 30 and 40 °C while keeping other conditions the same. Different from the conclusion of Bassin *et al.* (2011), in this study, as shown in Figure 4(a), the ammonium adsorption capacity of AGS was decreased from 2.03 to 1.36 mgNH_4^+-N/gTSS while the temperature was increased from 10 to 40 °C, leading to a 7% decrease in adsorption efficiency (AE), indicating that the ammonium adsorption process is exothermic and high temperature has a negative effect on it. This may be caused by the weakness of the bonding force between ammonium and adsorption sites while the thermal motion of ammonium ions is agitated at high temperature (Saltali *et al.* 2007).

To validate the adsorption type, thermodynamic parameters including the changes of free energy (ΔG^θ), enthalpy (ΔH^θ) and entropy (ΔS^θ) were analyzed from the equations that correlate with equilibrium constant (K_L) calculated by the Langmuir isotherm and temperatures (Equations (11) and (12)).

$$\Delta G^\theta = -RT\ln K_L \tag{11}$$

$$\ln K_L = -\frac{\Delta H^\theta}{RT} + \frac{\Delta S^\theta}{R} \tag{12}$$

where T is the temperature in Kelvin, R is the gas constant, 8.314×10^{-3} kJ/(mol · K) and K_L is the adsorption equilibrium constant (L/mol). The calculation of K_L at different temperature is shown in Table S4 and Figure S6 (available online).

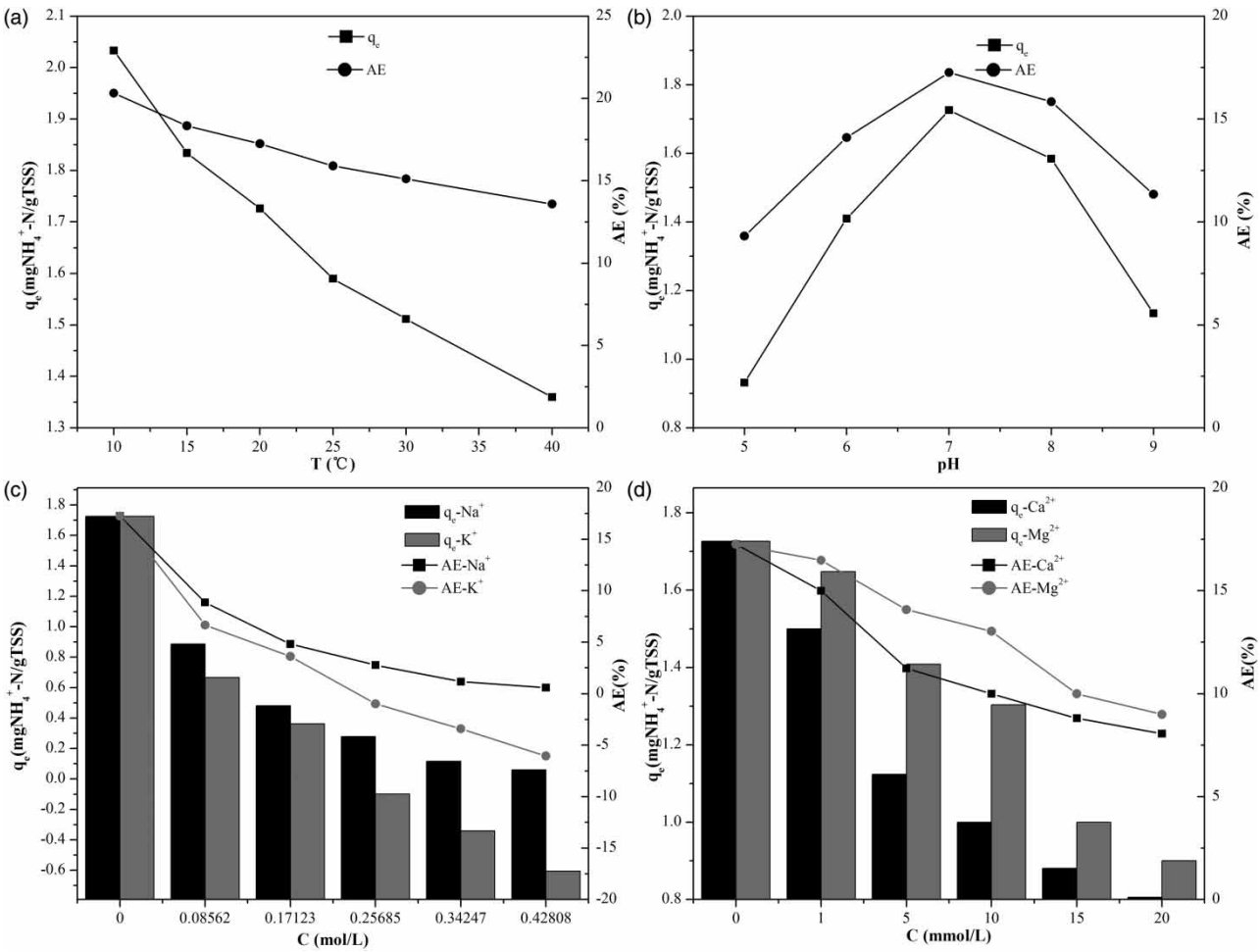

Figure 4 | The effect of (a) temperature, (b) pH, (c) K^+ and Na^+ and (d) Ca^{2+} and Mg^{2+} on ammonium adsorption.

We plotted $\ln K_L$ against T^{-1} and the fitting line is shown in Figure S7 (available online). Entropy and enthalpy of the adsorption process were calculated by the intercept and the slope of the fitting line. Values of thermodynamic parameters are summarized in Table 3. The changes of free energy at 283, 293 and 313 K are in the range of −12.86 to −12.64 kJ/mol, indicating that the ammonium adsorption process is spontaneous and physical ($0 > \Delta G^{\theta} > -20$ kJ/mol), with no need for energy input. The absolute values of free energy are decreased, suggesting that the increase in temperature is unfavorable for ammonium adsorption. The negative value of enthalpy indicates that the ammonium adsorption is exothermic. Therefore, ammonium ions would tend to escape from adsorption sites to the aqueous phase at high temperature. The negative value of entropy shows a decrease of randomness in the interface of solid/liquid during adsorption and also proves that the ammonium adsorption is thermal driving.

Effect of pH

To evaluate the effect of initial pH on the ammonium adsorption process, batch experiments were conducted in a pH range of 5–9, which are the values found in most wastewater effluent. Tris-HCl buffer was utilized to keep pH constant during adsorption. It was observed that the adsorption capacity increased when the initial pH of system was increased from 5 to 7, as shown in Figure 4(b), and the maximum adsorption capacity of 1.726 mgNH_4^+-N/gTSS was obtained at pH 7. A slight decrease of ammonium adsorption capacity was observed when the pH was increased from 7 to 9. Therefore, neutral pH was the best for ammonium adsorption in AGS.

Generally, pH can affect the adsorption process through controlling the surface charge of AGS, existing forms of ammonia nitrogen and H^+ concentrations in solution. The zeta-potential of EPS in AGS was negative, indicating that the surface charge of AGS is negative and the ammonium could be adsorbed by electrostatic interaction (Crini & Badot 2008). The transformation of ammonia nitrogen in solution can be described as: $NH_4^+ + OH^- \leftrightarrow NH_3 + H_2O$. When the solution is acid (pH < 7), it is mainly NH_4^+ which can be easily adsorbed by the adsorption sites, no matter whether through ion exchange or electrostatic interaction. However, the concentration of H^+ is high under such condition. Diffusion resistance of H^+ inside AGS is lower than that of NH_4^+ as the H^+ hydrated ionic radius is smaller (0.24 nm < 0.29 nm) (Karadag *et al.* 2007). Therefore, H^+ is more competitive for negative charged adsorption sites and the protonation of the surface groups occurs, reducing the electronegativity of AGS. The electronegativity of AGS is increased when pH > 7 because of a higher concentration of OH^- compared with acid condition and theoretical ion exchange rate should be improved. Nevertheless, the form of ammonia nitrogen converts from NH_4^+ to NH_3 under alkaline environment, which is impossible for ion exchange, resulting in the decline of ammonium adsorption capacity.

The rise of pH in the system was observed when Tris-HCl buffer was absent and pH was without control (shown in Figure S8, available online). It may be due to the cationic hydrolysis which was promoted by the adsorption of cations onto AGS, suggesting that the adsorption of ammonium in AGS could increase the alkalinity in solution, which may improve the ammonium removal rate by promoting nitrification.

Effect of co-existing metal cations

Four cationic salts, NaCl, KCl, $CaCl_2$ and $MgCl_2$, which are the most common cations in actual wastewater were employed to investigate the effect of competitive cations on ammonium adsorption. The concentrations of Na^+ and K^+ were in the range of 0 to 0.43 mol/L and Ca^{2+} and Mg^{2+} were 0 to 20 mmol/L, respectively, because the Na^+ and K^+ effect on ammonium adsorption was hard to distinguish at low concentrations. As shown in Figure 4(c) and 4(d), ammonium adsorption capacity is significantly affected by increasing the concentration of cations, decreasing from 1.726 mgNH_4^+-N/gTSS to 0.89, 0.67, 1.5 and 1.65 mgNH_4^+-N/gTSS at the concentration of 0.08 mol/L of Na^+ and K^+ and 1.0 mmol/L of Ca^{2+} and Mg^{2+},

Table 3 | Thermodynamic parameters for ammonium adsorption

T(k)	ΔG^{θ} (kJ/mol)	95% CI	ΔH^{θ} (kJ/mol)	95% CI	ΔS^{θ} (J/mol · K)	95% CI
283	−12.86	±1.25				
293	−12.68	±0.93	− 14.697	± 1.476	− 6.65	± 0.341
313	−12.64	±1.03				

respectively. When the concentrations of Ca^{2+} and Mg^{2+} are at 20 mmol/L and Na^{+} at 0.43 mol/L, ammonium adsorption capacity is decreased to 0.8, 0.9 and 0.06 mgNH_4^+-N/gTSS, respectively. The corresponding AE of ammonia was decreased about 9.2%, 8.3% and 16.7%, respectively. An increase of ammonium concentration in solution is observed when the K^{+} concentrations are higher than 0.25 mol/L. It is possible that the desorption rate is slow and a fraction of ammonium remained adsorbed on granules and then was extracted by KCl solution though ammonium in the liquid phase was completely depleted (Nielsen 1996).

The effect of co-existing cations on ammonium adsorption is in the order $Ca^{2+} > Mg^{2+} > K^{+} > Na^{+}$. Obviously, divalent cations are more competitive than monovalent cations, and more effective in neutralizing the negatively fixed-charge groups in the surface of AGS (Yang *et al.* 2014). The hydrated radius of Na^{+}, K^{+}, Ca^{2+} and Mg^{2+} is 0.358, 0.331, 0.412 and 0.428 nm (Tansel *et al.* 2006). When valence was the same, hydrated radius seemed to be the decisive factor since the diffusion might be easier inside AGS for smaller cations and there would be more chances to contact with adsorption sites.

Desorption properties

The desorption batch tests of AGS at different temperatures were carried out to determine the effect of temperature on the ammonium desorption process. The ammonium concentration (C_{eq}) in aqueous phase at desorption equilibrium and the corresponding desorption efficiency are shown in Figure S9 (available online). The adsorption of ammonium in AGS was shown to be reversible while the desorption rate reached 92.7% at 20 °C, which was also found in Bassin's research (Bassin *et al.* 2011). However, with the decrease of temperature, the desorption rate was decreased gradually. The C_{eq} and desorption efficiency were only 6.8 mgNH_4^+-N/L and 66.9% at 10 °C, indicating that varying temperature could significantly affect the desorption process. As the reverse process of ammonium adsorption, ammonium desorption from AGS should be endothermal while the adsorption process has been proved to be exothermal. Therefore, the desorption rate would be decreased at low temperature. This may also be one of the reasons for ammonium removal rate in the bioreactor to be unsatisfactory at low temperature besides low microbial activity, in which the high ammonium adsorption rate and low desorption rate lead to low ammonium transfer efficiency for ammonia-oxidizing bacteria, further reducing the ammonium oxidation rate.

CONCLUSION

Ammonium adsorption and desorption processes in AGS were investigated. Batch experiments showed that the adsorption process occurred quickly, reaching adsorption equilibrium within 60 min. Analysis of kinetics models indicated that ammonium adsorption was a pseudo-second-order reaction. Intra-particle diffusion studies indicated that the internal diffusion and surface adsorption controlled the adsorption rate. Langmuir, Freundlich and Temkin isotherm models were fitted to experimental data. The correlation coefficient showed that the Langmuir isotherm model described the adsorption process best and the maximal adsorption capacity was 4.95 mgNH_4^+-N/gTSS. The values of thermodynamic parameters ($\Delta H^{\theta} = -14.697$ kJ/mol, $\Delta S^{\theta} = -6.65$ J/(mol · K)) revealed that the ammonium adsorption in AGS was a spontaneous and exothermic process and low temperature could increase the adsorption capacity. Neutral environment was considered to be the optimum condition for ammonium adsorption. The effect of competitive cations was in the order $Ca^{2+} > Mg^{2+} > K^{+} > Na^{+}$. Desorption batch experiments demonstrated that the ammonium adsorption was reversible and high temperature could improve the ammonium desorption rate in AGS.

ACKNOWLEDGEMENTS

This research was supported financially by the Program of International S&I Cooperation (2016YFE0123400) and the National Natural Science Foundation of China (No. 51278143).

REFERENCES

Angar, Y., Djelali, N.-E. & Kebbouche-Gana, S. 2016 Kinetic and thermodynamic studies of the ammonium ions adsorption onto natural Algerian bentonite. *Desalination and Water Treatment* **57** (53), 25696–25704.

APHA 1998 *Standard Methods for the Examination of Water and Wastewater*, 20th edn. American Public Health Association/American Water Works Association/Water Environment Federation, Washington, DC, USA.

Arami, M., Limaee, N. & Mahmoodi, N. 2008 Evaluation of the adsorption kinetics and equilibrium for the potential removal of acid dyes using a biosorbent. *Chemical Engineering Journal* **139** (1), 2–10.

Bassin, J. P., Pronk, M., Kraan, R., Kleerebezem, R. & van Loosdrecht, M. C. 2011 Ammonium adsorption in aerobic

granular sludge, activated sludge and anammox granules. *Water Research* **45** (16), 5257–5265.

Corsino, S. F., Capodici, M., Morici, C., Torregrossa, M. & Viviani, G. 2016 Simultaneous nitritation-denitritation for the treatment of high-strength nitrogen in hypersaline wastewater by aerobic granular sludge. *Water Research* **88**, 329–336.

Crini, G. & Badot, P.-M. 2008 Application of chitosan, a natural aminopolysaccharide, for dye removal from aqueous solutions by adsorption processes using batch studies: a review of recent literature. *Progress in Polymer Science* **33** (4), 399–447.

de Kreuk, M. K., Heijnen, J. J. & van Loosdrecht, M. C. M. 2005 Simultaneous COD, nitrogen, and phosphate removal by aerobic granular sludge. *Biotechnology and Bioengineering* **90** (6), 761–769.

Drzewicki, A., Cydzik-Kwiatkowska, A. & Mieczkowski, D. 2017 Impact of high-nitrogen leachate on microfauna of aerobic granular sludge. *Water Environment Research* **89** (9), 890–895.

Gooddy, D. C., Lapworth, D. J., Bennett, S. A., Heaton, T. H., Williams, P. J. & Surridge, B. W. 2016 A multi-stable isotope framework to understand eutrophication in aquatic ecosystems. *Water Research* **88**, 623–633.

Hammaini, A., Gonzalez, F., Ballester, A., Blazquez, M. L. & Munoz, J. A. 2007 Biosorption of heavy metals by activated sludge and their desorption characteristics. *Journal of Environmental Management* **84** (4), 419–426.

Ho, Y. S. & McKay, G. 1999 Pseudo-second order model for sorption processes. *Process Biochemistry* **34** (5), 451–465.

Karadag, D., Koc, Y., Turan, M. & Ozturk, M. 2007 A comparative study of linear and non-linear regression analysis for ammonium exchange by clinoptilolite zeolite. *Journal of Hazardous Materials* **144** (1–2), 432–437.

Li, Y., Li, J., Zhang, Y., Wang, X. & Zheng, Z. 2016 Capability of ammonium adsorption by anaerobic ammonia oxidation granular sludge. *Water, Air, & Soil Pollution* **227** (8), 262.

Liu, Q.-S., Zheng, T., Wang, P., Jiang, J.-P. & Li, N. 2010 Adsorption isotherm, kinetic and mechanism studies of some substituted phenols on activated carbon fibers. *Chemical Engineering Journal* **157** (2–3), 348–356.

Mosquera-Corral, A., de Kreuk, M. K., Heijnen, J. J. & van Loosdrecht, M. C. 2005 Effects of oxygen concentration on N-removal in an aerobic granular sludge reactor. *Water Research* **39** (12), 2676–2686.

Nielsen, P. H. 1996 Adsorption of ammonium to activated sludge. *Water Research* **30**, 762–764.

Raji, C. & Anirudhan, T. S. 1998 Batch Cr(VI) removal by polyacrylamide-grafted sawdust: kinetics and thermodynamics. *Water Research* **32** (12), 3772–3780.

Saltali, K., Sari, A. & Aydin, M. 2007 Removal of ammonium ion from aqueous solution by natural Turkish (Yildizeli) zeolite for environmental quality. *Journal of Hazardous Materials* **141** (1), 258–263.

Schwitalla, P., Mennerich, A., Austermann-Haun, U., Muller, A., Dorninger, C., Daims, H., Holm, N. C. & Ronner-Holm, S. G. 2008 NH_4^+ ad-/desorption in sequencing batch reactors: simulation, laboratory and full-scale studies. *Water Science and Technology* **58** (2), 345–350.

Tansel, B., Sager, J., Rector, T., Garland, J., Strayer, R. F., Levine, L., Roberts, M., Hummerick, M. & Bauer, J. 2006 Significance of hydrated radius and hydration shells on ionic permeability during nanofiltration in dead end and cross flow modes. *Separation and Purification Technology* **51** (1), 40–47.

Van Loosdrecht, M. & Jetten, M. 1998 Microbiological conversions in nitrogen removal. *Water Science and Technology* **38** (1), 1–7.

Vishniac, W. & Santer, M. 1975 The thiobacilli. *Bacteriological Reviews* **18**, 195–213.

Wik, T. 1999 Adsorption and denitrification in nitrifying trickling filters. *Water Research* **9**, 1500–1508.

Yang, K., Zhang, X., Chao, C., Zhang, B. & Liu, J. 2014 In-situ preparation of NaA zeolite/chitosan porous hybrid beads for removal of ammonium from aqueous solution. *Carbohydrate Polymers* **107**, 103–109.

Zhang, L.-L., Feng, X. X., Xu, F., Xu, S. & Cai, W. M. 2005 Biosorption of rare earth metal ion on aerobic granules. *Journal of Environmental Science and Health, Part A* **40** (4), 857–867.

Zhao, Y., Zhang, B., Zhang, X., Wang, J., Liu, J. & Chen, R. 2010 Preparation of highly ordered cubic NaA zeolite from halloysite mineral for adsorption of ammonium ions. *Journal of Hazardous Materials* **178** (1–3), 658–664.

Zhou, M., Gong, J., Yang, C. & Pu, W. 2013 Simulation of the performance of aerobic granular sludge SBR using modified ASM3 model. *Bioresource Technology* **127**, 473–481.

Zou, J., Tao, Y., Li, J., Wu, S. & Ni, Y. 2018 Cultivating aerobic granular sludge in a developed continuous-flow reactor with two-zone sedimentation tank treating real and low-strength wastewater. *Bioresource Technology* **247**, 776–783.

First received 14 June 2018; accepted in revised form 14 September 2018. Available online 28 September 2018